Journal of Arid Environments 74 (2010) 579–584

Contents lists available at ScienceDirect

Journal of Arid Environments

journal homepage: www.elsevier.com/locate/jaridenv

Improved land–atmosphere relations through distributed footprint sampling in a subtropical scrubland during the North American monsoon

Enrique R. Vivoni [a,*], Christopher J. Watts [b], Julio C. Rodríguez [b], Jaime Garatuza-Payán [c], Luis A. Méndez-Barroso [a], Juan A. Sáiz-Hernández [b]

[a] Arizona State University, Tempe, AZ, USA
[b] Universidad de Sonora, Hermosillo, Sonora, Mexico
[c] Instituto Tecnológico de Sonora, Ciudad Obregón, Sonora, Mexico

ARTICLE INFO

Article history:
Received 29 January 2009
Received in revised form
15 September 2009
Accepted 23 September 2009
Available online 21 October 2009

Keywords:
Ecohydrology
Eddy covariance
Energy balance
Semiarid
Soil moisture
Sonoran desert

ABSTRACT

The relation between land surface states and fluxes is fundamental for quantifying the ecohydrological controls on the North American monsoon. In this study, we utilize distributed sampling around an eddy covariance tower in Sonora, México, to evaluate the impact of footprint variations in soil moisture (θ) and temperature (T_s) on surface flux partitioning. Results indicate that spatial variability is important to capture when θ or T_s have a high spatial mean and control the dominant surface flux, either latent (λE) or sensible (H) heat. As a result, we found that θ and T_s measurements at the tower may not be representative of the footprint-averaged states, with larger discrepancies for T_s due to the radiative heterogeneity. Using the spatially-averaged land surface conditions in the footprint moderately improves the relations with the surface fluxes as quantified by the Bowen ratio (B) and the evaporative fraction (EF). To our knowledge, this is a first attempt to address the scale discrepancy between aggregated flux measurements from an eddy covariance tower and the effective land surface states within the footprint through distributed sampling. Improvements in land–atmosphere relations are more significant for footprint conditions exhibiting high spatial variability or a large bias as compared to the tower site measurements.

1. Introduction

Land surface conditions or states are hypothesized to control the partitioning of sensible (H) and latent heat (λE) fluxes over a range of different climate settings (e.g., Alfieri et al., 2007; Blanken et al., 2001; Williams and Albertson, 2004). For example, soil moisture (θ) exerts control on the amount of evapotranspiration (ET) in the North American monsoon (NAM) region as quantified using the eddy covariance (EC) technique (Vivoni et al., 2008a). Typically, EC measurements aggregate turbulent fluxes within a time-variable footprint around the tower and thus represent spatially-averaged exchanges between the land and atmosphere (e.g., Detto et al., 2006; Li et al., 2008). In theory, aggregated turbulent fluxes derived from the EC technique should be compared to the 'effective' or spatially-averaged land surface conditions within the EC footprint. In practice, however, a small number of land surface measurements, such as soil moisture, are collected at the tower site (e.g., Running et al., 1999; Watts et al., 2007; Williams and Albertson, 2004), ignoring the land surface states within the EC footprint but further from the tower. To our knowledge, the scale discrepancy between the spatially-averaged (or aggregated) EC fluxes in the tower footprint and the point-scale land surface states near the tower has not been previously addressed. One approach to remedy this situation is through distributed footprint sampling of land surface conditions around an EC tower.

Water-limited ecosystems are potentially more vulnerable to the mismatch between tower flux and land surface measurements due to their heterogeneous vegetation composition. In the NAM region, for example, ecosystems are composed of mixtures of different plant types and bare soil (Caso et al., 2007; Trejo and Dirzo, 2002; Vivoni et al., 2007). As a result, quantification of land surface states should account for the complex assemblage of vegetated and bare patches. In another heterogeneous landscape, Detto et al. (2006) described an approach for characterizing conditions around an EC tower through high-resolution (2.8 m) thermal imagery. Surface temperature (T_s) data were then used with a footprint model (Hsieh et al., 2000) to decompose the aggregated EC flux and estimate the

* Corresponding author at: School of Earth and Space Exploration and School of Sustainable Engineering and the Built Environment, Arizona State University, Bateman Physical Sciences Center, F-Wing, Room 650-A, Tempe, AZ 85287, USA. Tel.: +1 480 965 5228; fax: +1 480 965 8102.
E-mail address: vivoni@asu.edu (E.R. Vivoni).

0140-1963/$ – see front matter © 2009 Elsevier Ltd. All rights reserved.
doi:10.1016/j.jaridenv.2009.09.031

relation between ET and θ for individual patches. In this study, we explore an alternative approach accounting for the spatial patterns of land surface states (T_s and θ) through distributed measurements in the EC tower footprint.

The relation between aggregated fluxes and effective states is important since the footprint area for spatial averaging becomes more comparable to the resolutions of numerical model forecasts and remote sensing observations. As a result, this relation could be used to test prognostic models of land–atmosphere interactions (Gutzler et al., 2005) or to derive additional variables from remote sensing data (Timmermans et al., 2007). In addition, simple relations between surface fluxes and states at the footprint-scale may be useful for minimalistic models (Juang et al., 2007) of land–atmosphere interactions. Given the dramatic vegetation seasonality during the NAM (Watts et al., 2007), this relation should vary with ecosystem composition and its dynamics. Here, we demonstrate that footprint-averaged surface conditions improve the relation with aggregated EC fluxes in a subtropical scrubland experiencing seasonal greening during the North American monsoon. This finding is potentially useful for the design of land–atmosphere studies in a range of other climate settings and landscape conditions.

2. Materials and methods

Our focus in this study is on EC tower flux and land surface measurements at the Rayón site (latitude 29.74°N, longitude 110.54°W) in northern Sonora, México (Fig. 1). The site is located at ~632 m above sea level in the Río San Miguel, a large ephemeral river basin (~3796 km^2) flowing north to south in the Sierra Madre Occidental (SMO, Vivoni et al., 2007). Site vegetation is classified as a subtropical scrubland (STS) or Sinaloan thornscrub (Brown, 1994), and is a mixture of trees, shrubs, cacti, grasses and bare soil that responds vigorously to precipitation during the NAM. Areally-extensive subtropical scrublands are found at intermediate elevations in the SMO (CEC, 1997; Fig. 1a). As the only EC tower in the STS ecoregion, the Rayón site is an important site to quantify the dynamics of ecosystems experiencing vegetation greening during the NAM.

Subtropical scrublands are typically associated with complex terrain having moderate slopes (Brown, 1994). Accordingly, the Rayón EC tower was placed on a flat alluvial fan surface dissected by small, ephemeral channels (Fig. 1b). Moderate relief in the vicinity of the tower (or footprint) leads to variations in vegetation cover, including higher plant density along the channels. Dominant species include mesquite (*Prosopis juliflora*), whiteball acacia (*Acacia angustissima*), tree ocotillo (*Fouquieria macdougalii*) and palo verde (*Cercidium sonorae*). Soil profiles are shallow (~70 cm above a hard clay lens) and sandy loam in texture with intermixed clasts. Shallower soil layers above more developed clay horizons are found closer to the ephemeral channels. Additional details on the study site can be found in Watts et al. (2007) and Vivoni et al. (2008a).

To quantify the land surface conditions around the EC tower, we established twenty-nine sampling plots in an area of ~250 m by 250 m in a grid pattern with ~50 m spacing between plots (Fig. 1b). This sampling region was selected to: (1) encompass the typical EC footprint areas found in prior studies (e.g., Horst and Weil, 1994; Hsieh et al., 2000), and (2) to match the pixel resolution of the MODIS (Moderate Resolution Imaging Spectroradiometer) reflectance measurements at 250 m. While we recognize that the surface flux footprint varies with wind conditions, stability and roughness properties, the sampling design allows for a set of repeatable land surface measurements. Each sampling plot (~1 m by 1 m) was sampled at similar times each day during approximately a two-week period in July 2006, 2007 and 2008 for a total of 38 sampling dates (see Table 1).

Land surface measurements at the sampling plots were performed using hand-held instruments over local times ranging from 8:00 am to 11:00 am. Volumetric soil moisture (θ in %) was sampled over 0–6 cm using an impedance (or Theta) probe (Cosh et al., 2005), while soil temperature (T_s in °C) was measured at three depths (~1, 5 and 10 cm) with a hand-held digital soil

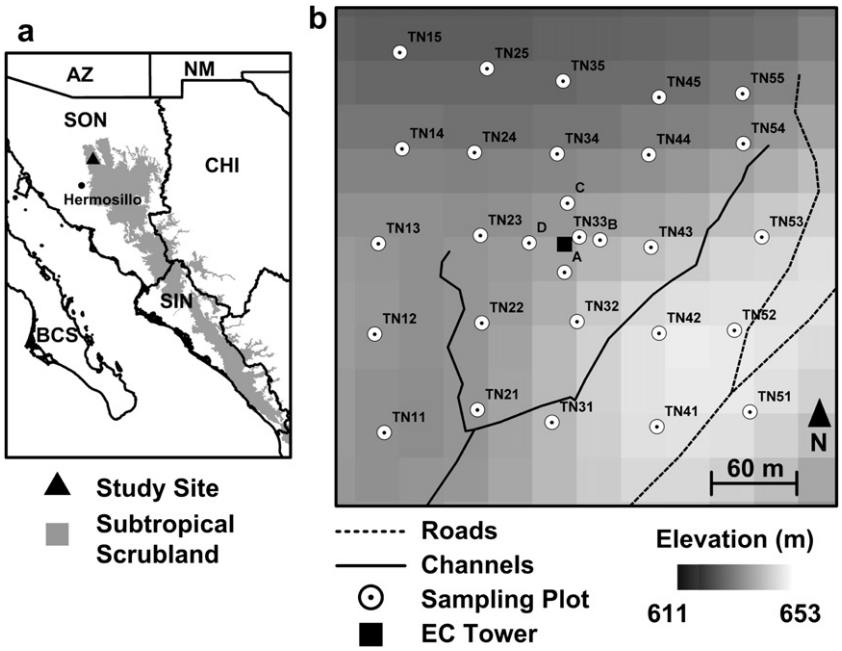

Fig. 1. (a) Study site in Rayón, Sonora, México within the subtropical scrubland ecoregion (total area of ~79,000 km^2). (b) Twenty-nine sampling plots in a 250 m box surrounding the EC tower overlain on a 30 m Digital Elevation Model (DEM) derived from ASTER (Advanced Spaceborne Thermal Emission and Reflection Radiometer). The roads and ephemeral channels were traced in the field using a global positioning system.

Table 1
Sampling characteristics, including lengths of tower and footprint measurements (DOY = day of year) and common period (days) used in Fig. 4. Precipitation (P in mm) refers to the accumulated rainfall during DOY 183–200 in 2006, 200–214 in 2007, and 181–200 in 2008. $\langle\overline{\theta}\rangle$ and $\langle\overline{T_s}\rangle$ are space–time averages; and $\sigma(\overline{\theta})$ are $\sigma(\overline{T_s})$ are the spatial variability of the temporal averages at all sites.

Year	Tower period (DOY)	Footprint period (DOY)	Common period (days)	P (mm)	$\langle\overline{\theta}\rangle$ (%)	$\sigma(\overline{\theta})$ (%)	$\langle\overline{T_s}\rangle$ (°C)	$\sigma(\overline{T_s})$ (°C)
2006	189–233	187–200	12	89.2	9.69	2.55	32.84	3.17
2007	151–240	204–214	10	73.7	9.19	1.87	29.74	2.20
2008	185–253	185–199	10	184.4	10.79	2.30	31.28	1.88

thermometer. Five sets of readings were taken daily in each plot with the Theta probe and soil thermometer to obtain plot-averaged soil moisture (averaged quantity over the 0–6 cm depth) and soil temperature (at the three depths). This strategy captured the variability of a soil variable within each plot (via the five measurements) and in the EC tower footprint (via the different locations). Furthermore, the sampling plots captured the spatial variations of terrain, vegetation and soil properties to ensure that effective land surface conditions in the footprint were obtained through simple (arithmetic) averaging. While simultaneous measurements at all plots were not possible within the footprint, the use of two sampling teams during the morning (8:00–11:00 am) helped to minimize the effects of the diurnal cycle, in particular for soil temperature which exhibits higher diurnal changes as compared to soil moisture.

Footprint sampling was carried out during periods of coincident measurements at the EC tower. The instrument package on the tower contains a CSAT3 (Campbell Scientific) three-dimensional sonic anemometer, a L17500 (LI-COR) hygrometer and a CNR1 (Kipp & Zonen) net radiometer to perform high-frequency sampling of wind speed, air temperature, specific humidity and net radiation at 9 m measurement height. As described fully in Watts et al. (2007), the measurements were used to estimate the sensible (H) and latent heat (λE) fluxes. Here, we used daily values of H and λE (MJ/day) to obtain the Bowen ratio ($B = H/\lambda E$) and evaporative fraction ($EF = \lambda E/(H + \lambda E) = 1/(1 + B)$). Procedures for analyzing the EC tower data are described in Scott et al. (2004). Other observations at the site include precipitation (P) from a tipping bucket rain gauge.

3. Results

3.1. Temporal variations in footprint-scale conditions

Fig. 2 presents the temporal variation of the volumetric soil moisture (0–6 cm depth) and soil temperature (1 cm depth) in the EC tower footprint for the three sampling periods. In the following, the EC footprint is assumed to consist of the 250 m box around the tower containing the 29 sampling plots, which is sufficiently large to encompass typical time-variable footprint areas (e.g., Horst and Weil, 1994). Footprint-averaged conditions ($\langle\theta\rangle$ and $\langle T_s\rangle$, where angle brackets are spatial averages) are represented by symbols, while the footprint variability ($\sigma(\theta)$ and $\sigma(T_s)$, where σ is the spatial standard deviation) are denoted by vertical bars. Daily rainfall (P) provides a context for interpreting the temporal changes in land surface conditions. As expected, $\langle\theta\rangle$ increases after rain events and decreases during interstorm periods. The storm sequence also provides an indication of radiative control on soil temperature. Increasing $\langle T_s\rangle$ with time is typically associated with clear days, while constant $\langle T_s\rangle$ is likely for cloudy days. Footprint-scale soil moisture also impacts soil temperature, with decreasing $\langle T_s\rangle$ during wet periods and vice versa. While the inverse correlation between $\langle T_s\rangle$ and $\langle\theta\rangle$ is statistically significant ($\langle T_s\rangle = -0.37\langle\theta\rangle + 35.20$, $R^2 = 0.29$, $F < 0.0005$ at $\alpha = 0.05$), the moderate R^2 indicates that other radiative factors, such as cloudiness and tree shading, also influence the soil temperature.

A comparison of the sampling periods in Fig. 2 does not reveal significant year-to-year changes in footprint-scale soil moisture and soil temperature conditions. For example, the space-time average values ($\langle\overline{\theta}\rangle$ and $\langle\overline{T_s}\rangle$, where overbars are time averages) and standard deviations ($\sigma(\overline{\theta})$ and $\sigma(\overline{T_s})$) in Table 1 are similar among the years. The minimum and maximum values of $\langle\theta\rangle$ and $\langle T_s\rangle$ are also similar among the sampling periods. In addition, these statistics follow expected trends with the observed rainfall (P) during the sampling periods, with the exception of $\langle\overline{T_s}\rangle$ in 2007, which was affected by persistent cloudiness. Consistency among the years is primarily due to timing the sampling after the NAM onset, thus avoiding the dramatic transition between pre-monsoon and NAM periods, as described in Watts et al. (2007). As a result, temporal variations in footprint-scale conditions are a function of rainfall and solar radiation, with smaller effects from the degree of vegetation development (see Vivoni et al., 2008a).

The spatial variability of land surface conditions within the footprint is depicted in Fig. 2 by the vertical bars. Overall, sampling days with high θ or T_s tend to exhibit greater spatial variations under these conditions, consistent with other studies in semiarid sites (e.g., Martínez and Ceballos, 2003; Vivoni et al., 2008b). This is confirmed by strong positive relations between the spatial means and standard deviations: $\sigma(\theta) = 0.11\langle\theta\rangle + 1.73$ ($R^2 = 0.42$, $F < 10^{-5}$ at $\alpha = 0.05$) and $\sigma(T_s) = 0.35\langle T_s\rangle - 8.1$ ($R^2 = 0.58$, $F < 10^{-8}$ at $\alpha = 0.05$). Note that the low significance F values (less than 0.05 at the 95% confidence interval, $\alpha = 0.05$) indicate a statistically significant relation among the variables. As a result, spatial differences in the footprint are more pronounced for greater T_s or θ. Since T_s and θ are closely related (e.g., Lakshmi et al., 2003), hot and dry days lead to high $\sigma(T_s)$ and low $\sigma(\theta)$, while cool and wet days have low $\sigma(T_s)$ and high $\sigma(\theta)$. This suggests that spatial patterns in θ are important to represent during cool, wet days (when λE is high and soil moisture is more variable), while spatial variations in T_s are more important for hot, dry days (with high H and soil temperature is more variable). As a consequence, distributed footprint sampling of a particular land surface state is warranted when the variable (soil moisture or soil temperature) exhibits high values and controls the dominant surface flux (latent or sensible heat flux), as discussed in the following.

3.2. Tower representativeness of footprint-scale conditions

Given the spatial variations evident in the distributed sampling, it is critical to assess if tower measurements of soil moisture and temperature are representative of the effective or spatially-averaged land surface states. Fig. 3 compares the footprint-scale conditions with measurements near the tower site at plot TN33 (~1.5 m distant, Fig. 1b) obtained using similar sampling methods. Perfect agreement between the point and spatially-averaged observations is represented by the 1:1 lines (solid black). Clearly, the correspondence between the footprint-scale and tower measurements is moderate for soil moisture, but low for soil temperature conditions. In both cases, the resulting linear regressions between point and spatially-averaged values (dashed lines) are statistically significant: $\langle\theta\rangle = 0.83\theta_T + 1.39$ ($R^2 = 0.83$, SEE = 1.92%, $F < 10^{-15}$ at $\alpha = 0.05$) and $\langle T_s\rangle = 0.58T_{sT} + 11.94$ ($R^2 = 0.64$, SEE = 3.45 °C, $F < 10^{-8}$ at $\alpha = 0.05$), where θ_T and T_{sT} are tower site values and SEE is the standard error of estimate. This indicates the tower site moderately captures the effective soil moisture averaged over the footprint, but misrepresents the footprint-scale soil temperature, in particular for hotter conditions. This

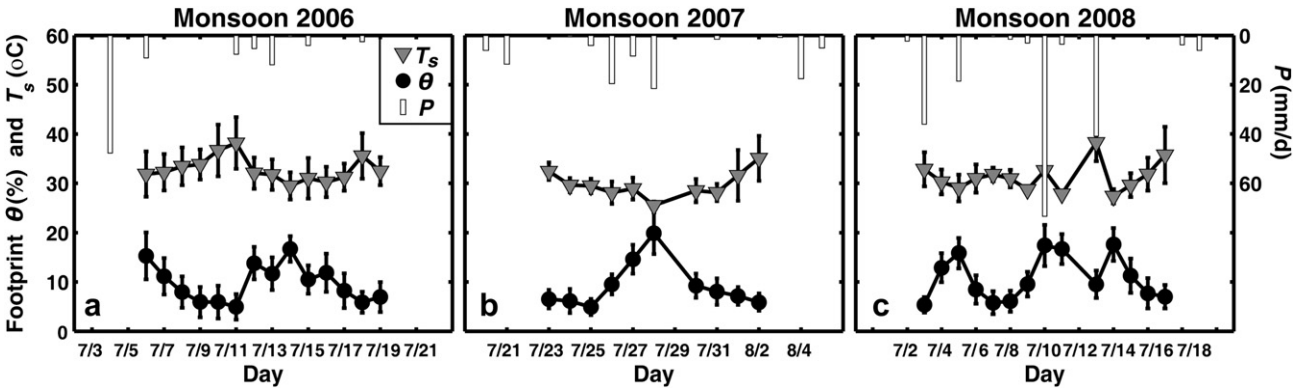

Fig. 2. Temporal variations in footprint-scale volumetric soil moisture (θ in %), soil temperature (T_s at 1 cm depth in °C) and daily precipitation (P in mm/day) for: (a) Monsoon 2006 (DOY 187–200), (b) Monsoon 2007 (DOY 204–214) and (c) Monsoon 2008 (DOY 185–199). Symbols represent the daily footprint spatial average (29 sampling plots), while the bars depict the ±1 spatial standard deviation.

suggests that greater footprint heterogeneity is present for soil temperature, potentially due to variations in radiative forcing from tree shading and cloudiness.

The above-cited comparisons, however, are a result of using all sampling days from multiple years. For an individual day, the discrepancy between point and footprint-averaged soil moisture and soil temperature can be as high as 4.2% and 7.4 °C, respectively. In addition, interannual variations in the point-to-area comparisons of soil moisture (Fig. 3a) and soil temperature (Fig. 3b) are observed. For example, wetter footprint conditions occur, on average, in 2006 (+1.42%), while drier spatially-averaged values are observed in 2008 (−1.39%), as compared to the tower site. Correspondingly, the footprint-averaged soil temperatures are significantly lower, on average, in 2006 (−4.3 °C), in relation to the tower plot. This analysis cautions against assuming that EC tower measurements of land surface conditions are representative of the effective footprint values at timescales ranging from days to weeks. In this comparison, the correspondence between point and spatially-averaged data improved for soil moisture when considering all sampling days. As a result, single point data at EC sites do not appear to capture the spatiotemporal variability of footprint conditions at short timescales, though the long-term (climatological) variability is likely represented well.

3.3. Relation between footprint-scale conditions and surface fluxes

Based on the observed scale discrepancies, it is important to identify if effective footprint-scale conditions improve the relationships between surface fluxes and land surface states. Fig. 4 presents a comparison between the Bowen ratio (B) and the soil moisture values at the tower plot and averaged over the EC footprint. We elected to show the comparison between B and θ_T or $\langle\theta\rangle$ to establish a simple power-law relation, though a similar analysis can be performed for EF = $1/(1+B)$, as in Dirmeyer et al. (2000). As expected, B decreases with higher θ, indicating that λE becomes a more dominant term for wet conditions. This is illustrated through a power-law regression ($B(\theta) = a\theta^b$, where a and b are parameters) for the tower and footprint relations: $B(\theta_T) = 2.86\theta_T^{-0.61}$ ($R^2 = 0.26$, RMSE = 0.37, $F < 0.0005$ at $\alpha = 0.05$) and $B(\langle\theta\rangle) = 4.08\langle\theta\rangle^{-0.78}$ ($R^2 = 0.30$, RMSE = 0.36, $F < 0.0005$ at $\alpha = 0.05$). Both relations are statistically significant at the 95% confidence interval. Note that a and b for the $B(\langle\theta\rangle)$ relation are larger in magnitude, indicating that the effective footprint conditions are more strongly related to the surface flux partitioning. Use of the footprint-averaged soil moisture improves the form of $B(\theta)$ relation as compared to the tower data, in particular by modifying high soil moisture values that exhibit a larger footprint variability.

Despite the improvement obtained through footprint sampling, considerable variations exist in the $B(\theta)$ relation using the multiple sampling periods. For individual years, the power-law regression improves in 2006 and 2007 (Table 2), though not in 2008, indicating a stronger control of footprint-averaged soil moisture for these periods. The high coefficient of determination ($R^2 = 0.63$ and 0.81) suggests that a simple relation between B and $\langle\theta\rangle$ may exist. Note that the regression for 2007 excludes one outlier ($B = 1.88$, $\langle\theta\rangle = 9.51\%$) affected by cloudy conditions that limited λE. The weaker relation in

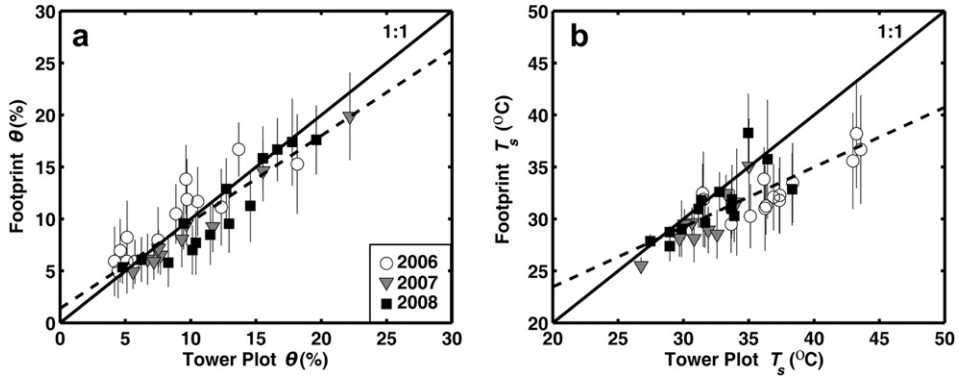

Fig. 3. Relation between footprint-scale conditions and measurements at tower site for all sampling days. (a) Volumetric soil moisture (θ in %). (b) Soil temperature (T_s at 1 cm depth in °C). Symbols represent the daily footprint average and the plot average at TN33, while the vertical bars depict the footprint variability (±1 spatial standard deviation).

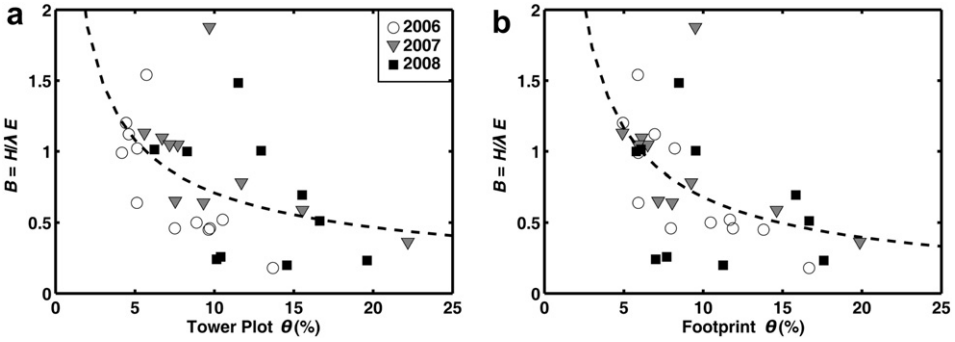

Fig. 4. Relation between volumetric soil moisture (θ in %) and the Bowen ratio ($B = H/\lambda E$) for common sampling days. (a) Tower plot measurements. (b) Footprint-averaged conditions. Dashed lines represent power-law regressions (see text for details).

2008 is due to three days ($B = \sim 0.2$–0.26, $\langle\theta\rangle = \sim 7$–$11\%$), where λE remains high after a rainfall event (July 13, 2008, Fig. 2), but the soil layer (0–6 cm) has dried. While this storm (>40 mm/d) led to deep infiltration (>30 cm), as confirmed by soil sampling, high solar radiation after the event quickly dried the surface. The lower than expected B (high λE) may indicate a period of time when tree transpiration from deeper (wet) soil layers within the EC footprint continued in spite of the drier surface layer. This period of high transpiration from deep soil layers resulted in a higher temporal variability in B and EF for 2008 (Table 2), as compared to the other years, which did not experience significant wetting to depths below 30 cm. In addition, the lower B and higher EF observed during 2008 are consistent with the higher rainfall and soil moisture within the footprint.

We also inspected the relationships between surface flux partitioning and soil temperature measured at the tower and averaged over the footprint (not shown). A weak negative relation between EF and T_S is present in both cases indicating that H increases slightly with soil temperature. The linear regression is moderately stronger for the footprint-averaged $\langle T_S\rangle$ as compared to the tower data: $\mathrm{EF} = -0.006T_{ST} + 0.80$ ($R^2 = 0.04$, RMSE = 0.14, $F < 0.30$ at $\alpha = 0.05$) and $\mathrm{EF} = -0.01\langle T_S\rangle + 0.99$ ($R^2 = 0.08$, RMSE = 0.13, $F < 0.11$ at $\alpha = 0.05$). However, the significance F value reveals that the two regressions are not significant at the 95% confidence interval. The minor improvement for the footprint relation is due to the effect of averaging soil temperatures over the footprint, in particular for high T_S (low EF) where the footprint is significantly cooler than the tower site. While these relations are much weaker than $B(\theta)$, the improvement obtained when using $\langle T_S\rangle$ lends further support to the importance of footprint sampling. In summary, the impacts of distributed sampling on the surface flux partitioning are more important when the following is observed: (1) high spatial variability in the land surface state, or (2) a large bias between the tower and the footprint-averaged states.

4. Discussion and conclusions

Quantifying how land surface states impact the partitioning of surface fluxes is critical for identifying terrestrial effects on the NAM (Higgins and Gochis, 2007; Vera et al., 2006). Nevertheless, the importance of measuring land surface conditions within an EC tower footprint has received little attention in land–atmosphere studies. Detto et al. (2006) and Chen et al. (2008), for example, addressed the spatial variability of surface conditions through remote sensing data and limited spatial data. In this study, we present a sampling strategy useful for intensive campaigns around EC towers in a range of climate or landscape settings. The distributed footprint observations provide important insights into the ecohydrological dynamics in a subtropical scrubland in the North American monsoon region. These include:

(1) An increase in the footprint spatial variability of soil moisture for wet conditions and in soil temperature for hot conditions (and vice versa).
(2) A discrepancy between the land surface conditions measured at the tower site and the effective states within the footprint at the daily and weekly scales.
(3) An improvement in the land–atmosphere relations when considering the footprint-scale conditions, in particular when large spatial variations or a high bias exist.

While feasible within short periods, the distributed sampling could be replaced with automated stations for long-term, high temporal resolution observations of rainfall, solar radiation, soil moisture and soil temperature. If sited to represent the heterogeneity in the EC footprint, this network could be used in the framework of a time-variable footprint model (e.g., Hsieh et al., 2000) to relate the surface fluxes to a weighted land surface condition obtained from the relevant sites. Automated observations at multiple soil depths could also be used to construct improved relations between surface flux partitioning and land surface states which may exhibit less unexplained variability. Further improvements in estimating the observed land–atmosphere relations in the NAM region would be helpful in modeling efforts addressing the ecohydrological role in precipitation generation and recycling (e.g., Dominguez et al., 2008; Juang et al., 2007).

Table 2
Characteristics of the surface flux partitioning during individual years: temporal mean and standard deviation of the Bowen ratio (B) and evaporative fraction (EF); and power-law regression statistics between B and (a) the footprint-averaged soil moisture $\langle\theta\rangle$ and (b) the tower soil moisture θ_T. The significance F statistic shows statistically significant relations for 2006 and 2007, but not 2008.

Year	$B(-)$		EF(−)		$B(\langle\theta\rangle)$; $B(\theta_T)$				
	Mean	Std	Mean	Std	a	b	R^2	RMSE	Significance F
2006	0.76	0.41	0.60	0.13	7.70; 5.60	−1.12; −1.08	0.63; 0.61	0.26; 0.26	$<5\times10^{-4}$; $<3\times10^{-4}$
2007	0.92	0.42	0.54	0.11	4.04; 4.11	−0.78; −0.74	0.81; 0.75	0.13; 0.15	<0.04; <0.03
2008	0.66	0.45	0.64	0.16	2.61; 3.85	−0.61; −0.72	0.13; 0.16	0.44; 0.43	<0.40; <0.24

Acknowledgements

We acknowledge funding from the NOAA Climate Program Office (GC07-019), the NSF IRES Program (OISE 0553852) and the U.S. Fulbright Program. We also thank the numerous undergraduate and graduate students and researchers from the U.S. and Mexico who participated in the distributed field sampling: T. Meixner, J. Zarate, J.B.J. Harrison, J. Kleissl, E.A. Yepez, M. Gurrola, A. Robles, G. Mascaro, M. Gebremichael, S. Yatheendradas, S. Archer, R. O'Keefe, A. Martinez, W. DeFoor, J. Craft, K. Bandy, T. Dotson, F. Di Benedetto, L. Liuzzo, L. Martini, L. Alvarez, L. De La Cruz, S. Padilla, S. Naif, J. Luna, N. Rodriguez, D. Martinez, J. Navarro, J. Cuevas, M. Molina, J. Gutierrez, J. Velazquez, E. Valenzuela, M. Valenzuela, C. Galaviz, T. Tarin, J. Esquer, E. Perez, B. Rivera, J. Benitez, K. Gutierrez, M. Varela and J. Arellano.

References

Alfieri, J.G., Blanken, P.D., Yates, D.N., Steffen, K., 2007. Variability in the environmental factors driving evapotranspiration from a grazed rangeland during severe drought conditions. Journal of Hydrometeorology 2, 207–220.

Blanken, P.D., Black, T.A., Neumann, H.H., den Hartog, G., Yang, P.C., Nesic, Z., Lee, X., 2001. The seasonal water and energy exchange above and within a boreal aspen forest. Journal of Hydrology 245, 118–136.

Brown, D.E., 1994. Biotic Communities Southwestern United States and Northwestern Mexico. University of Utah Press, Salt Lake City, UT.

Caso, M., González-Abraham, C., Ezcurra, E., 2007. Divergent ecological effects of oceanographic anomalies on terrestrial ecosystems of the Mexican Pacific coast. Proceedings of the National Academy of Sciences 104, 10530–10535.

CEC, 1997. Ecological Regions of North America. Commission for Environmental Cooperation, Montreal, Canada.

Chen, X., Rubin, Y., Ma, S., Baldocchi, D., 2008. Observations and stochastic modeling of soil moisture control on evapotranspiration in a California oak savanna. Water Resources Research 44, W08409. doi:10.1029/2007WR006646.

Cosh, M.H., Jackson, T.J., Bindlish, R., Famiglietti, J.S., Ryu, D., 2005. Calibration of an impedance probe for estimation of surface soil water content over large regions. Journal of Hydrology 311, 49–58.

Detto, M., Montaldo, N., Albertson, J.D., Mancini, M., Katul, G., 2006. Soil moisture and vegetation controls on evapotranspiration in a heterogeneous Mediterranean ecosystem on Sardinia, Italy. Water Resources Research 42, W08419. doi:10.1029/2005WR004693.

Dirmeyer, P.A., Zeng, F.J., Ducharne, A., Morrill, J.C., Koster, R.D., 2000. The sensitivity of surface fluxes to soil water content in three land surface schemes. Journal of Hydrometeorology 1, 121–134.

Dominguez, F., Kumar, P., Vivoni, E.R., 2008. Precipitation recycling variability and ecoclimatological stability – a study using NARR data. Part II: North American monsoon region. Journal of Climate 21, 5187–5203.

Gutzler, D.S., Kim, H.K., Higgins, R.W., Juang, H., Kanamitsu, M., Mitchell, K., Mo, K., Pegion, P., Ritchie, E., Schemm, J.K., Schubert, S., Song, Y., Yang, R., 2005. The North American monsoon model assessment project. Bulletin of the American Meteorological Society 86, 1423–1429.

Higgins, W., Gochis, D., 2007. Synthesis of results from the North American Monsoon Experiment (NAME) process study. Journal of Climate 20, 1601–1607.

Horst, T.W., Weil, J.C., 1994. How far is far enough?: the fetch requirements for micrometeorological measurement of surface fluxes. Journal of Atmospheric and Oceanic Technology 11, 1018–1025.

Hsieh, C.I., Katul, G., Chi, T., 2000. An approximate analytical model for footprint estimation of scalar fluxes in thermally stratified atmospheric flows. Advances in Water Resources 23, 765–772.

Juang, J.Y., Katul, G.G., Porporato, A., Stoy, P.C., Siquiera, M.S., Detto, M., Kim, H.S., Oren, R., 2007. Eco-hydrologic controls on summertime convective rainfall triggers. Global Change Biology 13, 887–896.

Lakshmi, V., Jackson, T.J., Zehrfuhs, D., 2003. Soil moisture–temperature relationships: results from two field experiments. Hydrological Processes 17, 3041–3057.

Li, F., Kustas, W.P., Anderson, M.C., Prueger, J.H., Scott, R.L., 2008. Effect of remote sensing spatial resolution on interpreting tower-based flux observations. Remote Sensing of Environment 112, 337–349.

Martínez, J., Ceballos, A., 2003. Temporal stability of soil moisture in a large-field experiment in Spain. Soil Science Society of America Journal 67, 1647–1656.

Running, S.W., Baldocchi, D.D., Turner, D.P., Gower, S.T., Bakwin, P.S., Hibbard, K.A., 1999. A global terrestrial monitoring network integrating tower fluxes, flask sampling, ecosystem modeling and EOS satellite data. Remote Sensing of Environment 70, 108–127.

Scott, R.L., Edwards, E.A., Shuttleworth, W.J., Huxman, T.E., Watts, C.J., Goodrich, D.C., 2004. Interannual and seasonal variations of fluxes of water and carbon dioxide from a riparian woodland ecosystem. Agricultural and Forest Meteorology 122, 65–84.

Timmermans, W.J., Kustas, K.J., Anderson, M.C., French, A.N., 2007. An intercomparison of the surface energy balance algorithm for land (SEBAL) and the two-source energy balance (TSEB) modeling schemes. Remote Sensing of Environment 108, 369–384.

Trejo, I., Dirzo, R., 2002. Floristic diversity of Mexican seasonally dry tropical forests. Biodiversity and Conservation 11, 2063–2084.

Vera, C., Higgins, W., Amador, J., Ambrizzi, T., Garreaud, R., Gochis, D., Gutzler, D., Lettenmaier, D., Marengo, J., Mechoso, J., Nogues-Paegle, J., Silva Dias, P.L., Zhang, C., 2006. Toward a unified view of the American monsoon systems. Journal of Climate 19, 4977–5000.

Vivoni, E.R., Gutiérrez-Jurado, H.A., Aragón, C.A., Méndez-Barroso, L.A., Rinehart, A.J., Wyckoff, R.L., Rodríguez, J.C., Watts, C.J., Bolten, J.D., Lakshmi, V., Jackson, T.J., 2007. Variation of hydrometeorological conditions along a topographic transect in northern Mexico during the North American monsoon. Journal of Climate 20, 1792–1809.

Vivoni, E.R., Moreno, H.A., Mascaro, G., Rodriguez, J.C., Watts, C.J., Garatuza-Payan, J., Scott, R.L., 2008a. Observed relation between evapotranspiration and soil moisture in the North American monsoon region. Geophysical Research Letters 35, L22403. doi:10.1029/2008GL036001.

Vivoni, E.R., Gebremichael, M., Watts, C.J., Bindlish, R., Jackson, T.J., 2008b. Comparison of ground-based and remotely-sensed surface soil moisture estimates over complex terrain during SMEX04. Remote Sensing of Environment 112, 314–325.

Watts, C.J., Scott, R.L., Garatuza-Payan, J., Rodríguez, J.C., Prueger, J.H., Kustas, W.P., Douglas, M., 2007. Changes in vegetation condition and surface fluxes during NAME 2004. Journal of Climate 20, 1810–1820.

Williams, C.A., Albertson, J.D., 2004. Soil moisture controls on canopy-scale water and carbon fluxes in an African savanna. Water Resources Research 40, W090302. doi:10.1029/2004WR003208.